Dense Amorphous Zirconia-Alumina by Low Temperature Consolidation of Spray Pyrolyzed Powders

Ashutosh S. Gandhi, Vikram Jayaram* and Atul H. Chokshi*

Department of Metallurgy, Indian Institute of Science, Bangalore - 560 012, India.

Abstract

Hot-pressing of metastable amorphous ZrO_2-Al_2O_3 powders was performed at low temperatures (873 and 923 K), under moderately high pressures (500 and 750 MPa), and amorphous pellets with 1 to 8 % porosity were obtained. Crystallization of the amorphous pieces between 1173 and 1673 K produced a range of ultrafine microstructures, the finest of which had 6-8 nm grains of tetragonal (ZrO_2-40 mol% Al_2O_3) solid solution formed at 1173 K. Sub-micron grain sizes of the equilibrium m-ZrO_2 and α-Al_2O_3 are stable against coarsening at 1673 K. The new technique was applied to produce a silicon carbide reinforced composite with an amorphous ZrO_2-80 mol% Al_2O_3 matrix; the high matrix sinterability overcame the reinforcement constraint. The results suggest a possible solution to the difficulties in bulk processing of amorphous, nanocrystalline and other novel ceramics.

Based on a poster presented at Ceramics Processing '97, Santa Barbara, CA, USA (September, 1997).

Supported by: (a) Department of Science and Technology, India; (b) Asian Office of Aerospace Research and Development, Tokyo (AFOSR, USA); (c) Department of Atomic Energy, India through 'Dr. K.S. Krishnan Fellowship' to A.S.G.

* Member, American Ceramic Society.

I. Introduction

Metastable ceramics produced by non-equilibrium processing techniques such as rapid solidification[1,2] and chemical precursor synthesis[3] have been known to possess interesting and potentially useful properties such as hard or soft magnetic characteristics, semiconductivity, varistor action and optical transmittivity. Apart from possessing attractive properties, a metastable phase may serve as a precursor to a desired microstructure; for instance, controlled crystallization of an amorphous phase is a route to produce a nanocrystalline structure.[4] Nanocrystalline ceramics are being widely studied because of their potential for novel functional and mechanical properties.[4-6] Among the various attractive properties, the possibility of superplasticity at high strain-rate and/or low temperature has spurred many research activities concerning the processing of nanocrystalline ceramics.

In order to study and utilize the nanostructured and other metastable ceramics extensively, it is important to synthesize these in bulk, dense form with control on the fine scale of the structure. Such efforts have not been entirely successful. Consolidation of particulate nanocrystalline and other metastable ceramics into dense forms requires activation in the form of high temperature, static or dynamic loading, or a combination of these. Such activation also triggers transformation to a more stable phase and grain growth,[7-20] leading to the loss of the initial desired structure by the time full density is attained. On the other hand, conditions that allow the desired metastable phase or nanometric grain size to be retained may not be adequate for complete densification. In the present study, the understanding of metastable phase synthesis and characteristics[3,21-26] was applied to the hot-pressing of amorphous ZrO_2-Al_2O_3 powders produced by spray pyrolysis in order to identify a pressure-temperature window in which consolidation would be possible without losing the metastable amorphous phase.

(1) Metastability in Spray-pyrolyzed ZrO_2-Al_2O_3

Spray pyrolysis is a route to the synthesis of amorphous and other metastable phases in ceramics at relatively low temperatures (1100 K and less).[3,27] Owing to such low temperature of synthesis, the equilibrium state can be kinetically suppressed and the system may evolve through many metastable states.[22]

Studies on metastable microstructures in the ZrO_2-Al_2O_3 powders produced by spray pyrolysis of aqueous zirconium acetate and aluminum nitrate solutions[23,24] established that the product of spray pyrolysis was amorphous for all compositions. On the ZrO_2-rich end, up to 40 mol% Al_2O_3, a single phase nanocrystalline tetragonal (t) $ZrO_2(Al_2O_3)$ solid solution crystallized upon heating the amorphous powder. With 40 mol% Al_2O_3, the phase evolution with temperature (K) was as follows:

$$\text{Amorphous} \xrightarrow{\sim 1143\,K} \text{t-}ZrO_2(Al_2O_3) \xrightarrow{\sim 1273} t\text{-}ZrO_2 + \gamma\text{-}Al_2O_3 \xrightarrow{\sim 1673} m\text{-}ZrO_2 + \alpha\text{-}Al_2O_3$$

where m denotes monoclinic. The grain sizes remained smaller than 100 nm after holding at 1273 K for up to 100 h, indicating the stability of the ultrafine microstructure.[24]

(2) Background to Hot-pressing of Amorphous ZrO_2-Al_2O_3

In previous hot-pressing experiments[25,26] on spray pyrolyzed amorphous ZrO_2-40 mol% Al_2O_3 under 1 GPa hydrostatic pressure, it was observed that the high pressure accelerated the formation of crystalline phases that are more dense and closer to equilibrium. Thus, a sample pressed at 973 K was already crystalline, partitioned to some extent and nearly fully dense. In contrast, another sample pressed at 1173 K consisted of the equilibrium m-ZrO_2 and α-Al_2O_3 phases and was significantly porous. These results imply that the farther the phases are from equilibrium, the better is the densification in spite of the substantially lower temperature. Also, the theory of nucleation applied to the transformation

of a parent phase, crystalline or amorphous, into a denser phase predicts that pressure is less effective in accelerating nucleation at lower temperatures.[26]

In the present study, hot-pressing experiments were performed at comparatively lower temperatures (873 and 923 K) and pressures (500 and 750 MPa) in an attempt to prevent crystallization of the amorphous phase and yet provide enough activation to the densification process in the amorphous powder compact. As described below, our attempts were successful in producing dense amorphous compacts of ZrO_2-Al_2O_3, with up to 99% relative density. The dense amorphous compacts were heat treated to produce nanocrystalline microstructures, demonstrating the feasibility of producing bulk nanocrystalline ceramics through this route.

The new processing route involving hot-pressing of a metastable amorphous phase was employed to overcome the well known problem of constrained sintering in ceramic composite processing.[28-31] The presence of non-sintering reinforcement particles retards the sintering rate of a conventional powder compact. In the present case, the constraint of the SiC reinforcement was overcome by the enhanced densification of the amorphous ZrO_2-Al_2O_3 phase during hot-pressing. The low temperature of densification (923 K) obviates the need for vacuum or inert atmosphere, as far as oxidation of SiC is concerned. The strong and refractory equilibrium matrix microstructure can be produced by heat treating after densification.

II. Experimental Procedure

(1) Production and Characterization of Amorphous Powders

Amorphous powders of composition ZrO_2-40 mol% Al_2O_3 (denoted as Z40A) and ZrO_2-80 mol% Al_2O_3 (Z80A) were obtained by spraying aqueous solutions containing both, zirconium nitrate and aluminum nitrate on to a Teflon coated pan held at 523 ± 10 K.

Composite powder (ZASC) with 7.7 wt% SiC_p dispersed in amorphous ZrO_2-80 mol% Al_2O_3 was produced by adding SiC particles smaller than 3μm to the spraying solution. Thermogravimetric analyses (CAHN TG-171) were performed on the as-sprayed Z40A and Z80A powders with a heating rate of 10 K/min. The temperature ranges of crystallization were identified by introducing as-sprayed powders into a furnace already heated to the desired temperature and removing it after certain duration (up-quenching). X-ray diffraction (JEOL, JDX-8030) was used to identify the phases present. Differential thermal analysis (Polymer Laboratories) at a heating rate of 10 K/min was carried out on as-sprayed Z40A powder to confirm the crystallization temperature.

The true densities of the amorphous phases obtained by pyrolysis of the as-sprayed Z40A powder by heating up to 1023 and 1073 K were measured by pycnometry using 25 ml specific gravity bottles and de-ionized water.[32] Weights of the bottles with powders and water were measured after allowing the water to fill all the inter-particle spaces by keeping the bottles in vacuum for 5 and 15 days, respectively, for the two powders. Effect of closed porosity was minimized by grinding the powders in an agate mortar and pestle.

(2) Hot-pressing

The starting powders and the conditions used for the consolidation experiments are listed in Table I. Hot-pressing was carried out on the as-sprayed agglomerated powders as well as those without the agglomerates. To produce de-agglomerated powders, the as-sprayed powders were first decomposed by holding at 1073 K for 1 hour so that all the volatile matter, except that retained till 1450K (see next section), was driven out. Agglomerates larger than ~10 μm were removed by sedimentation for 5 minutes in a 15 cm tall de-ionized water column, based on a true density of 3.3 g/cm^3 from pycnometry for Z40A. Settling time of 5.5 minutes was used for sedimenting ZASC, resulting in a finer powder.

A nickel base superalloy die with 5 mm internal diameter was used for consolidation in a screw driven universal testing machine (Instron) fitted with a furnace. Boron nitride powder was used for lubrication and 0.2 mm thick flexible graphite foils were used as spacers between the pellet and the punches. Cold compaction was done at 750 MPa.

Prior to hot-pressing, the green compacts of the as-sprayed Z40A powder were heated to 1023 K for 5 minutes to bring about the decomposition of the as-sprayed material and concurrent sintering. As reported earlier,[32] this step leads to higher starting densities prior to hot pressing, than compaction of decomposed powders. The compacts at this stage had relative densities of ~70-75%. After cooling to 873 or 923 K, a pressure of 500 or 750 MPa was applied for up to 90 minutes. The de-agglomerated powders were heated directly to 923 K and pressed at 750 MPa. In all the experiments, the heating and cooling rates were 20 to 30 K/min. The pressure was released before cooling to room temperature.

Porosity measurements by quantitative optical microscopy and Vickers hardness measurements (Shimadzu, HMV-2000) were made on the polished hot-pressed pellets.

(3) Crystallization of Hot-Pressed Pellets

Differential thermal analysis (DTA) was performed on a hot-pressed pellet from agglomerated powder to compare its crystallization behavior with the loose powder. Some of the hot-pressed samples were sectioned and the small pieces were subjected to crystallization by up-quenching for temperatures lower than 1273 K and by slow heating for higher temperatures up to 1673 K. Powder X-ray diffraction (XRD) patterns were taken from the heat treated pieces (HUBER Guinier Type 642). SEM (Scanning electron microscopy, JEOL, JSM-840A) was performed on samples heat treated to 1673 K after coating with carbon or gold. Image analysis was performed on the SEM micrographs from gold coated samples to measure the porosity introduced during crystallization.

III. Results and Discussion

(1) Powder Characteristics

The as-sprayed powders are highly agglomerated, with a primary particle size smaller than 10μm. Thermogravimetric analysis (TGA) of as-sprayed Z40A (Fig.1) shows that it loses ~25% weight by 520 K, which is due to the moisture absorbed during storage. Between 820 and 1020 K, a further loss of 2.7% occurs. The weight remains constant between 1020 and 1450 K with a final weight loss of 0.6% occurring around 1470 K. Fig.1 also shows that the Z80A powder loses more moisture up to 520 K. The second weight loss of 2.7% occurs over a larger temperature range of 920 to 1170 K while 0.9% weight is lost at ~1470 K.

The XRD patterns in Fig.2 show that the Z40A powder is amorphous after 5 minutes at 1133 K. The beginning of crystallization to t-ZrO_2 is noted after 5 minutes at 1153 K while well developed peaks appear at 1193 K. This temperature range corresponds to the sharp exotherm at 1188 K in the DTA curve (Fig.3). The phases α-Al_2O_3 and m-ZrO_2 appear at 1473 K although t-ZrO_2 is still the major phase. After heat treatments at 1573 K and 1673 K, the predominant phases are m-ZrO_2 and α-Al_2O_3 with some retained t-ZrO_2. The sequence of phase evolution is the same as that reported previously,[23,24] although the temperatures of appearance of the various phases are different.

The composition ZrO_2-80 mol% Al_2O_3 begins to crystallize at ~1173 K with the appearance of t-ZrO_2 peaks; γ-Al_2O_3 peaks appear at 1273 K while the equilibrium phases form at higher temperatures. The behavior of this Al_2O_3-rich composition is similar to the ZrO_2 rich end in so far as the amorphous phase is retained up to high enough temperatures to enable hot-pressing experiments to be carried out.

(2) Hot-pressing of Amorphous ZrO_2-40 mol% Al_2O_3

Table I summarizes the results of the hot-pressing experiments. The XRD pattern in Fig.4

from the Z40A pellet hot-pressed for the longest duration among these experiments (90 minutes) shows that it is amorphous. This result is corroborated by DTA carried out on a sample hot-pressed at 873 K (Fig.3), which reveals the same exotherm at 1173 K as seen in the case of the powder. Optical micrographs of the hot-pressed pellets from as-sprayed Z40A (Fig.5) show that significant densification occurs within 5 minutes of pressing at 923 K and 750 MPa. Since the as-sprayed powder is highly agglomerated, the hot-pressed pellets in Fig.5 have large voids (larger than 50μm) surrounding the regions of very low porosity. Porosity in these dense regions was measured by optical image analysis and is listed in Table I. No correlation is apparent between the time of hot-pressing and the final porosity, although the porosity after 90 minutes is the lowest in this set of experiments. Also, either a less severe pressure of 500 MPa or a lower temperature of 873 K does not appear to affect the densification process significantly. The large voids due to agglomeration may have masked the role of the hot-pressing parameters. However, these results also indicate the possibility that significant densification can occur at lower temperatures and pressures or in a short duration of a few minutes.

Hot-pressing of the decomposed, de-agglomerated powder yields a uniform distribution of fine porosity (Fig.6), measured to be 4%, including a few large pores (~50μm). The porosity distribution is fairly uniform throughout the pellet. It is observed that the overall porosity is sensitive to de-agglomeration. Complete pore elimination should therefore be possible by using finer amorphous powders (particles smaller than 1 μm), which can be accomplished in principle by comminution or by improving the spray pyrolysis technique.

Vickers hardness with 500 g load was measured on the Z40A samples and the values are listed in Table I. The measured hardness of the sample from de-agglomerated powder is much lower than those from the as-sprayed (agglomerated) powders. Owing to the uniform pore distribution in the sample from the de-agglomerated powder, more pores affected the

indentation compared to the pellets from agglomerated powder, for which the measurements were made on regions almost free of pores. Hence, the hardness measured on the sample pressed for 90 minutes, which has the lowest measured porosity, is taken as the hardness of the amorphous phase. It is lower by a factor of ~2.5 than the typical hardness value for partially stabilized ZrO_2 (~10 GPa) and by a factor of ~4.5 than that for α-Al_2O_3 (~18 GPa).

(3) Crystallization of Amorphous ZrO_2 -40 mol% Al_2O_3 Pellets

Crystallization of the amorphous hot-pressed pellets at 1173-1273 K, similar to that of the free, as-sprayed powder, produces t-ZrO_2(Al_2O_3) solid solution (Fig.4) with 6-8 nm grains measured from the broadening of the 111 peak and by the application of Scherrer's formula, after subtracting instrumental broadening. The exothermic peak in Fig.3(b) at 1178 K corresponds to crystallization. (A broad peak is seen at 664 K, the reasons for which are not known). The pellets developed additional porosity after crystallization; for instance, a sample heat treated at 1673 K for 2 hours contained ~31% porosity in regions that would be fully dense in the amorphous state. The size of these voids is a few hundred nanometers. The additional porosity is due to the large contraction expected from the molar volume difference between the amorphous and crystalline phases. After decomposition at 1073 K the density of the amorphous phase, as measured by pycnometry,[32] is 3.3 g/cm^3 which is 34% smaller than the density in the equilibrium state (5 g/cm^3 with m-ZrO_2 and α-Al_2O_3). As described earlier in this section, transformation to the equilibrium phases α-Al_2O_3 and m-ZrO_2 begins at 1473 K, at which stage the hot-pressed pellet has a ZrO_2 grain size of 100 nm. Table II and Fig.7 show that the microstructure consisting of m-ZrO_2, α-Al_2O_3 and some t-ZrO_2 remains sub-micrometer even after 1 hour at 1673 K. Such resistance to coarsening is characteristic of multiphase fine microstructures. These experiments demonstrate that a variety of fine microstructures can be produced in bulk form by suitably heat treating the dense amorphous

pellets. This route is easier to employ, particularly for multiphase ceramics, than currently available techniques that require the synthesis and mixing of nanoscale particles. This technique is similar to glass ceramics, although obtaining the stable amorphous phase is the difficult step in the present case.

(4) Hot-pressing of Amorphous ZrO_2-80 mol% Al_2O_3 Reinforced with 7.7 wt% SiC_p (ZASC)

The composition ZrO_2-80 mol% Al_2O_3 was chosen since it is close to the high Al_2O_3 range commercially used for its toughness and wear resistance. The volume fraction of SiC in the equilibrium microstructure would be 10%. De-agglomeration and hot-pressing were carried out similar to the ZrO_2 rich composition described earlier. The optical micrograph in Fig.8 shows porosity as low as 1% and a fairly uniform distribution of SiC in the hot-pressed composite. An important observation is that pores are distributed randomly, whereas in the conventionally processed α-Al_2O_3-SiC composite the pores are associated with the reinforcement[28,30]. These observations establish the possibility of producing fully dense ceramic composites at low temperatures by consolidation of an amorphous matrix that can be crystallized later into a tough, creep resistant microstructure. Conventional hot-pressing of mixture of α-Al_2O_3 and SiC powders is done at as high a temperature as 2100 K, in vacuum or inert atmosphere, at 25-50 MPa pressure. It may be noted that the present processing route obviates the need for vacuum and offers a reduction of over 1000 K over the temperatures used for commercial hot-pressing of SiC reinforced Al_2O_3 cutting tools.

A bulk processing route for metastable and nanocrystalline materials emerges from the results of hot-pressing experiments on amorphous ZrO_2-Al_2O_3 powders described above, which establish the good sinterability of the amorphous phases at temperatures lower than $0.4T_m$ with moderate pressures. The present results are distinct from other reports on

sintering with amorphous starting materials such as glass-ceramics,[33-39] amorphous mullite based powders,[10-12] amorphous Si-C-N[13-15,40] and Si-Zr-N-O powders.[41] The amorphous phases in the conventional glass and glass-ceramic systems are readily obtained from the molten states at ordinary cooling rates, and are sufficiently stable even above the glass transition temperatures so that sintering can take place through viscous flow of the supercooled liquid without crystallization.[35] Our results pertain to oxides that can be produced in the amorphous state only with special efforts, such as spray pyrolysis or rapid solidification, owing to the limited thermal stability of the amorphous phases with respect to crystalline phases. The presence of SiO_2 in mullite based materials makes the amorphous phases relatively easily accessible. Crystallization of mullite does not occur up to high homologous temperatures of ~$0.7T_m$ compared to $0.54T_m$ for ZrO_2-40 mol% Al_2O_3 (T_m is taken as the peritectic temperature for Al_2O_3-SiO_2 and as the eutectic temperature for ZrO_2-Al_2O_3 since the T_0 temperatures are not known). The mullite based systems thus have a larger temperature range in which sintering can occur prior to crystallization. The results of Jeng and Rahaman[11,12] on the sintering of amorphous mullite imply that the sintering kinetics are decelerated remarkably immediately upon crystallization, corroborating the observation that an amorphous phase is better sinterable than a crystalline phase and that conditions which retain the amorphous phase are favorable for densification. Experiments on the hot-pressing of amorphous Si-C-N powders at high temperatures of ~2020 K and pressures of ~30 MPa have produced Si_3N_4-SiC nano-composites with fine SiC grain sizes by crystallization of the amorphous phase during hot-pressing. It should be pointed out that except in the densification of glasses and glass-ceramics, the amorphous phase has so far not been retained after densification.

The present crystallization studies have established the wide range of bulk ultrafine microstructures that can be produced from the hot-pressed amorphous samples, although the

problem of de-sintering needs to be addressed. It may be possible to prevent opening of the porosity by applying pressure during crystallization. Vickers hardness measurements on the dense, amorphous ZrO_2-40 mol% Al_2O_3 samples are an example of bulk property measurements on metastable materials made possible by this synthesis route.

A possible reason for the high sinterability of amorphous phases in ZrO_2-Al_2O_3 system is indicated by the true density of the amorphous ZrO_2-40 mol% Al_2O_3 phase.[32] As described earlier, the density of the amorphous phase is only 66% of the density of the equilibrium microstructure. Moreover, ^{27}Al MAS-NMR spectroscopy on the ZrO_2-Al_2O_3 amorphous and crystalline solid solutions[26,42] have revealed the existence of 5-fold co-ordination of Al^{3+} with O^{2-} cations in addition to 4-fold and 6-fold co-ordinations. These observations, together with the low hardness of the amorphous material, imply that the amorphous phase has a more open structure compared to the equilibrium phases and is also likely to possess high concentrations of point defects due to non-stoichiometry and non-equilibrium processing conditions. Consequently, it may possess high ionic mobilities and low viscosity. At present these are unresolved issues. However, the present work is a successful application of the understanding of metastable phase synthesis and behavior to the production of novel ceramic microstructures in bulk form.

IV. Conclusions

1. Hot-pressing experiments on spray pyrolyzed amorphous ZrO_2-40 mol% Al_2O_3 powders at 873-923 K and 500-750 MPa have established that the amorphous powders have much greater sinterability than the equilibrium phases.
2. Hot-pressing of de-agglomerated (<10μm) powder produced a sample with uniformly distributed fine pores and a total porosity of only 4%.
3. The amorphous ZrO_2-40 mol% Al_2O_3 phase has a very low hardness of ~4.2 GPa,

compared to the equilibrium phases (more than 10 GPa for partially stabilized ZrO_2 and 18 GPa for α-Al_2O_3).

4. Heat treatment of the hot-pressed pellets produced a range of bulk ultrafine microstructures, the finest of which consists of a 6-8 nm tetragonal $ZrO_2(Al_2O_3)$ solid solution. The two-phase equilibrium microstructure is stable against rapid coarsening at 1673 K.
5. Hot-pressing of SiC_p reinforced amorphous ZrO_2-80 mol% Al_2O_3 produced a composite with only 1% porosity, demonstrating the potential of this processing route of hot-pressing an amorphous phase.
6. Low true density of the amorphous phase indicates an open structure and high point defect concentrations leading to high diffusivities and low viscosities, which may be the causes for the high sinterability of the amorphous phases.

Acknowledgements

The authors are grateful to Mr. Kaustubh Kulkarni for assistance in preparing the composite powders of ZrO_2-80% Al_2O_3 and SiC_p.

References

1. L.A. Jacobson and J. McKittrick, "Rapid Solidification Processing", *Mater. Sci. Eng.*, **R11**, 355-408 (1994).
2. M.C. Brockway and R.R. Wills, “Rapid Solidification of Ceramics, a Technology Assessment”, Report No. MCIC-84-49, Metals and Ceramics Information Center (1984).
3. C.G. Levi, “Metastability and Microstructure Evolution in the Synthesis of Inorganics from Precursors”, *Acta Mater.*, **46**, 787-800 (1998).
4. C. Suryanarayana, “Nanocrystalline Materials”, *Intl. Mater. Rev.*, **40**, 41-64 (1995).
5. H. Gleiter, “Materials with Ultrafine Microstructures: Retrospectives and Perspectives”,

Nanostructured Mater., **1**, 1-19 (1992).

6. R.W. Siegel, "Nanostructured Materials - Mind over Matter", *Nanostructured Mater.*, **3**, 1-18 (1995).
7. H. Watanabe, K. Hirota, O. Yamaguchi, S. Inamura, H. Miyamoto, H. Shiokawa and K. Tsuji, "Hot Isostatic Pressing of Tetragonal ZrO_2 Solid-Solution Powders Prepared from Acetylacetonates in the System ZrO_2-Y_2O_3-Al_2O_3", *J. Mater. Sci.*, **29**, 3719-23 (1994).
8. M. Fukuya, K. Hirota, O. Yamaguchi, H. Kume, S. Inamura, H. Miyamoto, N. Shiokawa and R. Shikata, "Sintering and Characterization of Yttria-Stabilized Zirconia with Alumina Derived from Solid Solution", *Mater. Res. Bull.*, **29**, 619-28 (1994).
9. J. McKittrick, B. Tunaboylu and J. Katz, "Microwave and Conventional Sintering of Rapidly Solidified Al_2O_3-ZrO_2 Powders", *J. Mater. Sci.*, **29**, 2119-25 (1994).
10. H. Ito, Y. Yamasaki, K. Takagi and H. Kuroki, "Effect of Zirconia Content on the Strength of Mullite Ceramics Hot-Pressed from Rapidly Solidified Powders', *J. Japan. Soc. Powder & Powder Met.*, **43**, 1466-72 (1996).
11. D.Y. Jeng and M.N. Rahaman, "Effect of Rigid Inclusions on the Sintering of Mullite Synthesized by Sol-Gel Processing", *J. Mater. Sci.*, **28**, 4421-26 (1993).
12. D.Y. Jeng and M.N. Rahaman, "Sintering and Crystallization of Mullite Powder Prepared by Sol-Gel Processing", *J. Mater. Sci.*, **28**, 4904-9 (1993).
13. T. Hirano, K. Niihara, T. Ohji and F. Wakai, "Improved Creep Resistance of Si_3N_4 Nanocomposites Fabricated from Amorphous Si-C-N Precursor Powder", *J. Mater. Sci. Lett.*, **15**, 505-7 (1996).
14. T. Hirano, K. Izaki and K. Niihara, "Microstructure and Thermal Conductivity of Si_3N_4/SiC Nanocomposites Fabricated from Amorphous Si-C-N Powders", *Nanostructured Mater.*, **5**, 809-18 (1995).
15. P. Sajgalik, J. Dusza, F. Hofer, P. Warbichler, M. Reece, G. Boden and J. Kozankova,

"Structural Development and Properties of SiC-Si_3N_4 Nano/Macro-Composites", *J. Mater. Sci. Lett.*, **15**, 72-6 (1996).

16. D.T. Castro and J.Y. Ying, "Synthesis and Sintering of Nanocrystalline Titanium Nitride", *Nanostructured Mater.*, **9**, 67-70 (1997).
17. D.-J. Chen and M.J. Mayo, "Rapid Rate Sintering of Nanocrystalline ZrO_2-3 mol% Y_2O_3", *J. Am. Ceram. Soc.*, **79**, 906-12 (1996).
18. M.J. Mayo, "Processing of Nanocrystalline Ceramics from Ultrafine Particles", *Intl. Mater. Rev.*, **41**, 85-115 (1996).
19. D.M. Owen and A.H. Chokshi, "An Evaluation of the Densification Characteristics of Nanocrystalline Materials", *Nanostructured Mater.*, **2**, 181-7 (1993).
20. D.J. Chen and M.J. Mayo, "Densification and Grain Growth of Ultrafine 3 mol% Y_2O_3-ZrO_2 Ceramics", *Nanostructured Mater.*, **2**, 469-78 (1993).
21. V. Jayaram, C.G. Levi, T. Whitney and R. Mehrabian, "Characterization of Al_2O_3-ZrO_2 Powders Produced by Electrohydrodynamic Atomization", *Mater. Sci. Eng.*, **A124**, 65-81 (1990).
22. V. Jayaram, M. de Graef, and C.G. Levi, "Metastable Extension of the Fluorite Phase Field in Y_2O_3-ZrO_2 and its Effect on Grain Growth", *Acta Metall. Mater.*, **42**, 1829-46 (1994).
23. M.L. Balmer, F.F. Lange and C.G. Levi, "Metastable Phase Selection and Partitioning for $Zr_{(1-x)}Al_{(2-x/2)}O_{(2-x/2)}$ Materials Synthesized with Liquid Precursors", *J. Am. Ceram. Soc.*, **77**, 2069-75 (1994).
24. M.L. Balmer, F.F. Lange, V. Jayaram and C.G. Levi, "Development of Nanocomposite Microstructures in ZrO_2-Al_2O_3 via the Solution Precursor Method", *J. Am. Ceram. Soc.*, **78**, 1489-94 (1995).
25. V. Jayaram, R.S. Mishra, B. Majumdar, C. Lesher and A.K. Mukherjee, "Dense

Nanometric ZrO_2-Al_2O_3 from Spray Pyrolysed Powder", *Colloids & Surfaces A*, **133**, 25-31 (1998)

26. R.S. Mishra, V. Jayaram, B. Majumdar, C. Lesher and A.K. Mukherjee, "ZrO_2-Al_2O_3 Nanocomposite by High Pressure Sintering of Spray Pyrolysed Powders", *J. Mater. Res.*, in press.
27. G.L. Messing, S.-C. Zhang and G.V. Jayanthi, "Ceramic Powder Synthesis by Spray Pyrolysis", *J. Am. Ceram. Soc.*, **76**, 2707-26 (1993).
28. A.S. Gandhi, A. Saravanan and V. Jayaram, "Containerless Processing of Ceramics by Aerodynamic Levitation", *Mater. Sci. Eng.*, **A221**, 68-75 (1996).
29. A. Jagota, "Simulation of Viscous Sintering of Coated Particles", *J. Am. Ceram. Soc.*, **77**, 2237-39 (1994).
30. C.-L. Fan and M.N. Rahaman, "Factors Controlling the Sintering of Ceramic Particulate Composites: I, Conventional Processing", *J. Am. Ceram. Soc.*, **75**, 2056-65 (1992).
31. R.K. Bordia and G.W. Scherer, "On Constrained Sintering - I. Constitutive Model for a Sintering Body", *Acta Metall.*, **36**, 2393-97, (1988).
32. A.S. Gandhi, V. Jayaram and A.H. Chokshi, "Phase Evolution and Densification of Spray Pyrolysed ZrO_2-Al_2O_3 Powders", *Materials Science Forum*, **243-245**, 227-32 (1997).
33. A.R. Boccaccini, D.H. Pearce and P.A. Trusty, "Pressureless Sintering and Characterization of Al_2O_3-Platelet Reinforced Barium-Magnesium Aluminosilicate Glass-Ceramic Composites", *Composites-A*, **28**, 505-10 (1997).
34. A.R. Boccaccini, W. Stumpfe, D.M.R. Taplin and C.B. Ponton, "Densification and Crystallization of Glass Powder Compacts During Constant Heating Rate Sintering", *Mater. Sci. Eng.*, **A219**, 26-31 (1996).
35. M.D. Glendenning and W.E. Lee, "Microstructural Development on Crystallizing Hot-

Pressed Pellets of Cordierite Melt-Derived Glass Containing B_2O_3 and P_2O_5", *J. Am. Ceram. Soc.*, **79**, 705-13 (1996).

36. M.J. Reece, C.A. Worrell, G.J. Hill and R. Morrell, "Microstructures and Dielectric Properties of Ferroelectric Glass-Ceramics", *J. Am. Ceram. Soc.*, **79**, 17-26 (1996).
37. I.A. Cornejo, J. Collier and M.J. Haun, "Ferroelectric and Crystallization Behavior in the $Pb_5Ge_3O_{11}$-$PbTiO_3$-$PbZrO_3$ Glass-Ceramic System", *Ferroelectrics*, **154**, 53-58 (1994).
38. E. Breval, M. Hammond and C.G. Pantano, "Nanostructural Characterization of Silicon Oxycarbide Glasses and Glass-Ceramics", *J. Am. Ceram. Soc.*, **77**, 3012-18 (1994).
39. B. Houng and M.J. Haun, "Lead Zirconate Titanate - Lead Silicate Piezoelectric Glass-Ceramics", *IEEE Intl. Symp. Applications of Ferroelectrics*, IEEE, Piscataway, NJ USA, **94CH3416-5**, 214-217 (1994).
40. W. Dressler and R. Riedel, "Progress in Silicon-Based Non-Oxide Structural Ceramics", *Intl. J. Refractory Met. Hard Mater.*, **15**, 13-47 (1997).
41. V.M. Sglavo, D.R. Maschio, G.D. Soraru and A. Bellosi, "Fabrication of Polymer-Derived Si_2N_2O-ZrO_2 Nanocomposite Ceramics", *J. Mater. Sci.*, **28**, 6437-41 (1993).
42. M.L. Balmer, H. Eckert, N. Das and F.F. Lange, "^{27}Al Nuclear Magnetic Resonance of Glassy and Crystalline $Zr_{(1-x)}Al_xO_{(2-x/2)}$ Materials Prepared from Solution Precursors", *J. Am. Ceram. Soc.*, **79**, 321-26 (1996).

Figure Captions

Fig.1: TGA plots for as-sprayed ZrO_2-Al_2O_3 powders. The weight remains constant from 1020 to 1450 K for Z40A and 1170 to 1450 K for Z80A. The phase evolution of the amorphous phases occurs in these temperature ranges of constant weight.

Fig.2: XRD patterns of Z40A powder heat treated at the indicated temperatures. The onset of crystallization is indicated by the advent of the 111 peak of tetragonal $ZrO_2(Al_2O_3)$.

Fig.3: DTA plots from (a) the as-sprayed Z40A powder and (b) a pellet hot-pressed at 873 K. The exotherms at 1173 K from both the materials coincide with the appearance of diffraction peak corresponding to {111} planes from tetragonal $ZrO_2(Al_2O_3)$ solid solution.

Fig.4: X-ray diffractograms of hot-pressed samples of Z40A. All the samples remain amorphous after hot-pressing. Amorphous phase crystallizes after heat treatment above 1173 K into tetragonal $ZrO_2(Al_2O_3)$ solid solution with 6-8 nm grains.

Fig.5: Optical micrographs of amorphous Z40A hot-pressed at 923 K and 750 MPa. (a) 5 minutes; (b) 90 minutes. The regions of low porosity form by densification of the agglomerates. The large pores are from voids between agglomerates.

Fig.6: The uniform pore distribution in this hot-pressed amorphous Z40A sample is due to the removal of agglomerates larger than ~10μm. The indication is that hot-pressing finer amorphous powders (particles smaller than 1 μm) may eliminate all the porosity.

Fig.7: Controlled heat treatment of hot-pressed amorphous pellet can lead to a wide range of desirable microstructures. Scanning electron micrograph of sub-micrometer grains of m-ZrO_2 (bright phase) and α-Al_2O_3 produced by heating a dense amorphous pellet of Z40A to 1673 K for 1 hour.

Fig.8: Optical micrograph of hot-pressed composite of amorphous ZrO_2-80 mol% Al_2O_3

reinforced with SiC particles (bright phase). This composite with only 1% porosity was produced at 923 K under 750 MPa pressure in air. Pores are randomly distributed whereas they surround the SiC in conventional processing[28,30].

Table I. Details of hot-pressing of amorphous spray pyrolyzed ZrO_2-Al_2O_3.

Composition	Starting Condition	Temperature (K)	Pressure (MPa)	Time (min.)	Porosity* (%)	Hardness (GPa)
Z40A	as-sprayed	923	750	5	4	3.2
Z40A	as-sprayed	923	750	30	4	3.4
Z40A	as-sprayed	923	750	60	8	-
Z40A	as-sprayed	923	750	90	2	4.2
Z40A	as-sprayed	923	500	60	4	2.8
Z40A	as-sprayed	873	750	60	4	-
Z40A	de-agglomerated	923	750	60	4	1.6
ZASC	de-agglomerated	923	750	60	1	-

* Except for the de-agglomerated samples, porosity was measured in the dense regions of the samples, i.e. excluding voids larger than ~50 μm.

Table II. Grain sizes in ZrO_2-40 mol% Al_2O_3 hot-pressed in the amorphous state and crystallized by heating as indicated.

Temperature (K)	Time (min.)	ZrO_2 Grain Size (nm)
1273	5	6*
1473	5	100†
1673	5	230†
1673	60	290†

***** Measured from XRD peak broadening.

† Measured from SEM image; mean intercept.

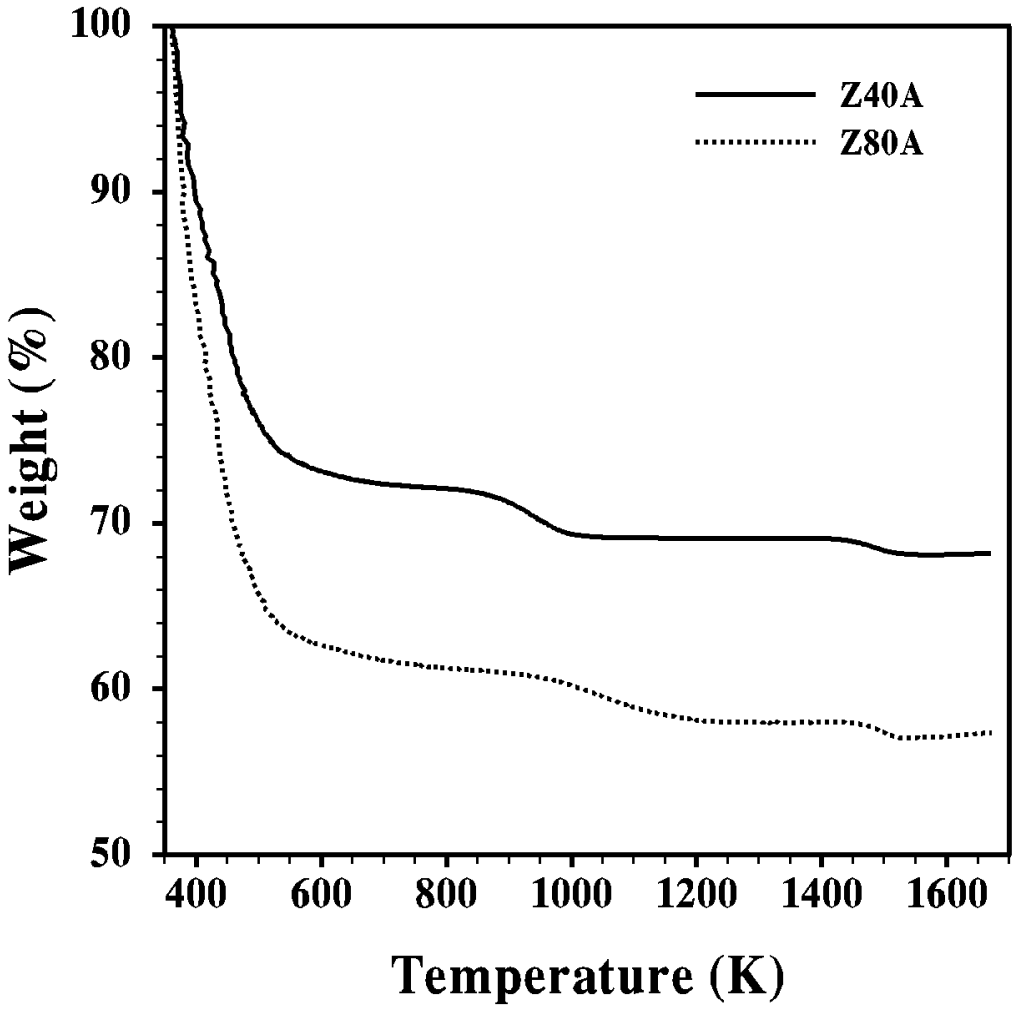

Fig.1: TGA plots for as-sprayed ZrO_2-Al_2O_3 powders. The weight remains constant from 1020 to 1450 K for Z40A and 1170 to 1450 K for Z80A. The phase evolution of the amorphous phases occurs in these temperature ranges of constant weight.

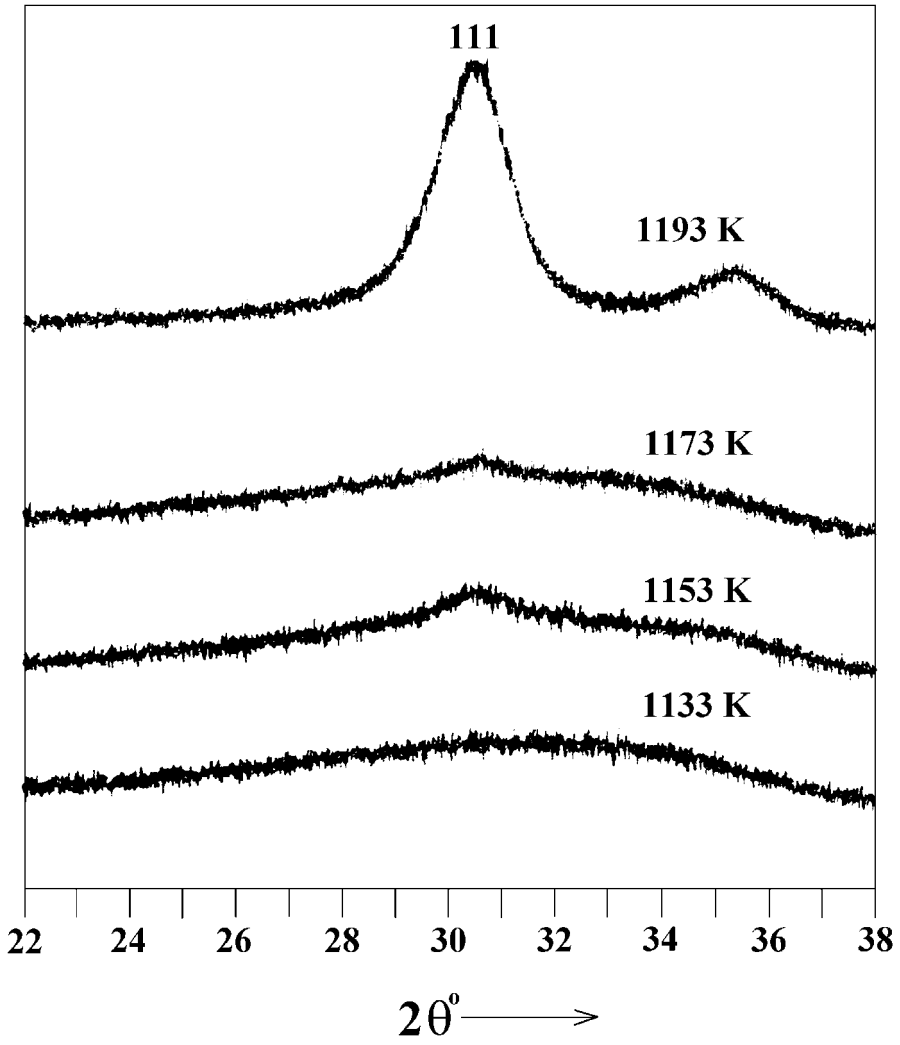

Fig.2: XRD patterns of Z40A powder heat treated at the indicated temperatures. The onset of crystallization is indicated by the advent of the 111 peak of tetragonal $ZrO_2(Al_2O_3)$.

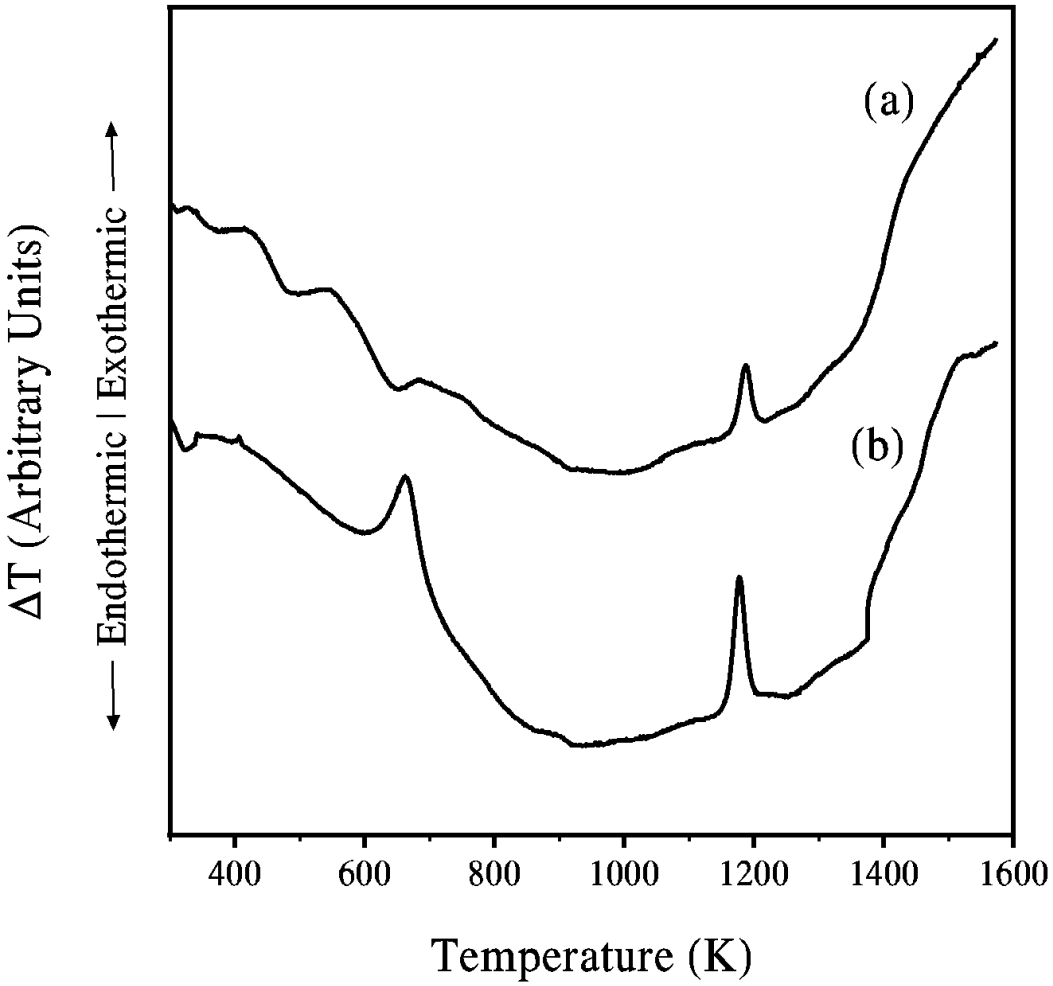

Fig.3: DTA plots from (a) the as-sprayed Z40A powder and (b) a pellet hot-pressed at 873 K. The exotherms at 1173 K from both the materials coincide with the appearance of diffraction peak corresponding to {111} planes from tetragonal $ZrO_2(Al_2O_3)$ solid solution.

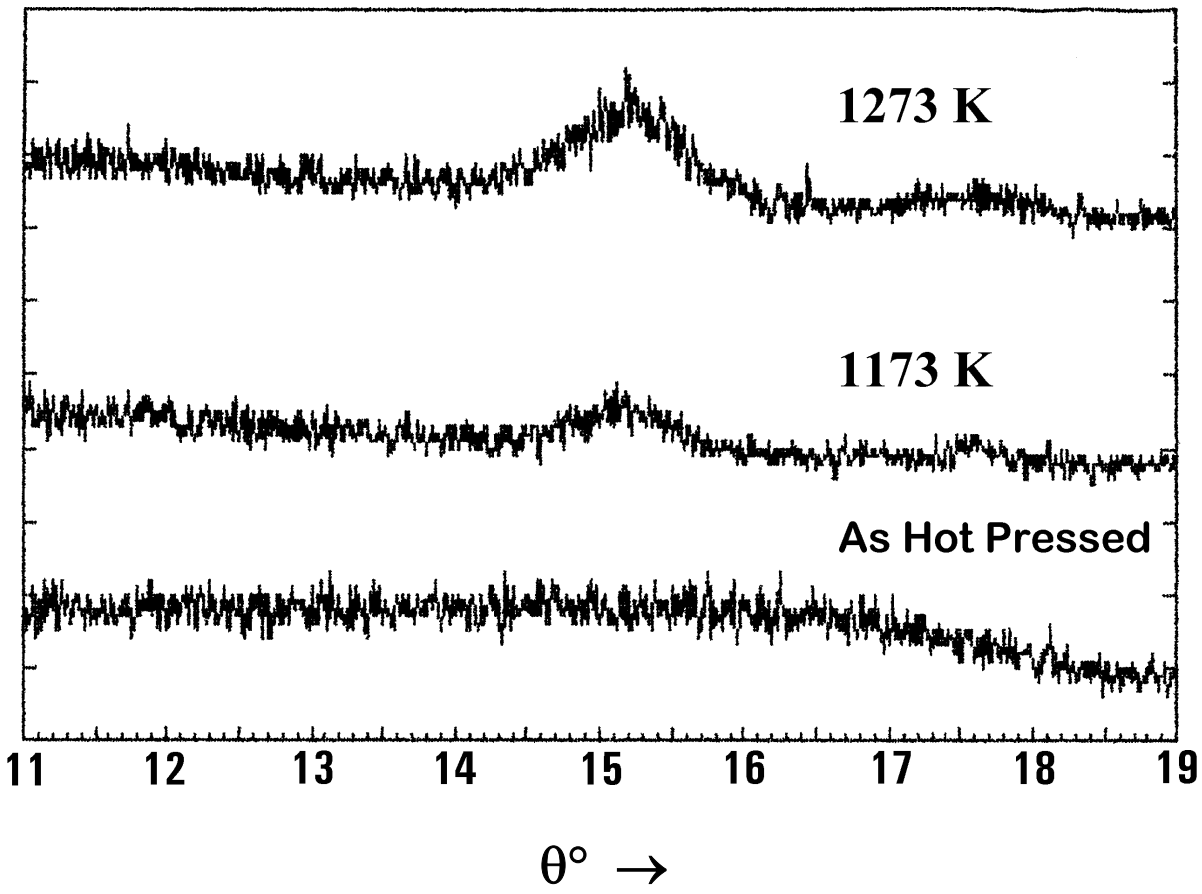

Fig.4: X-ray diffractograms of hot-pressed samples of Z40A. All the samples remain amorphous after hot-pressing. Amorphous phase crystallizes after heat treatment above 1173 K into tetragonal $ZrO_2(Al_2O_3)$ solid solution with 6-8 nm grains.

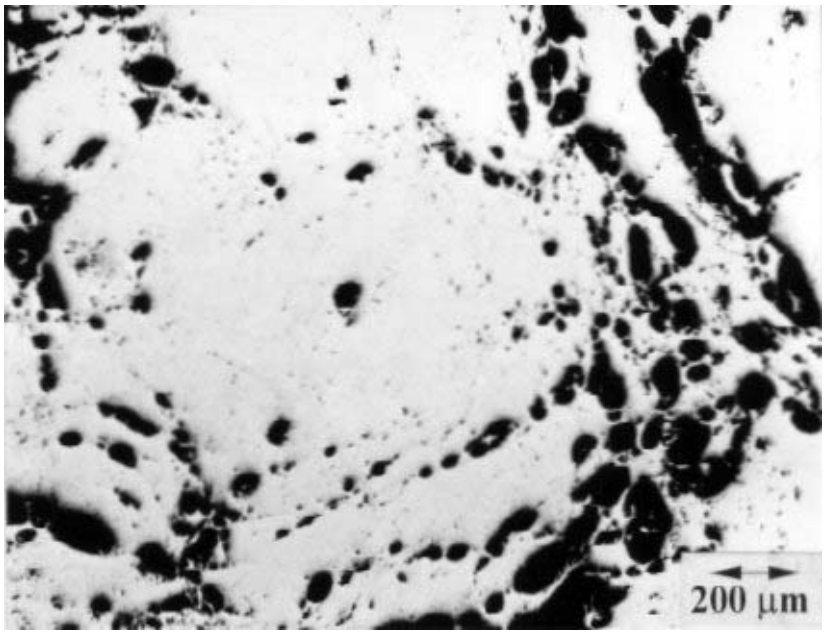

(a)

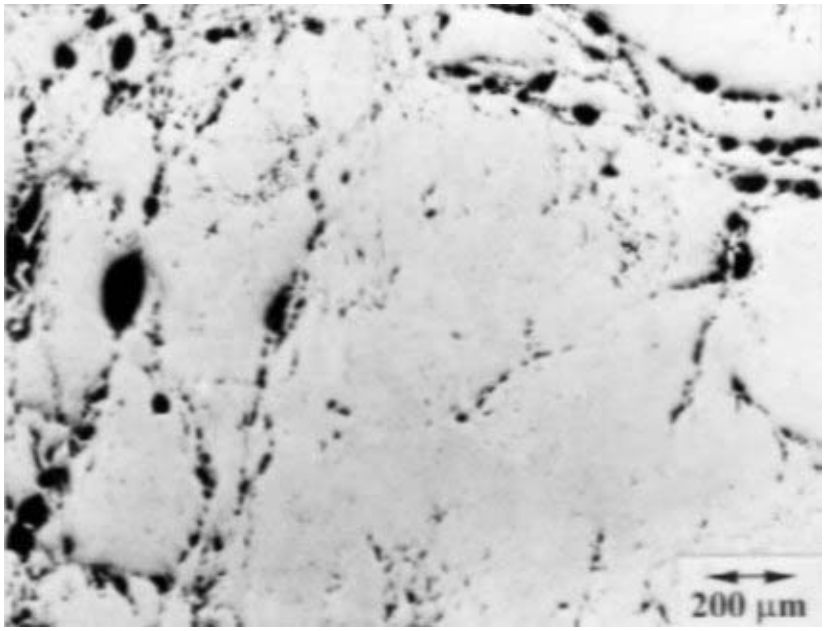

(b)

Fig.5: Optical micrographs of amorphous Z40A hot-pressed at 923 K and 750 MPa. (a) 5 minutes; (b) 90 minutes. The regions of low porosity form by densification of the agglomerates. The large pores are from voids between agglomerates.

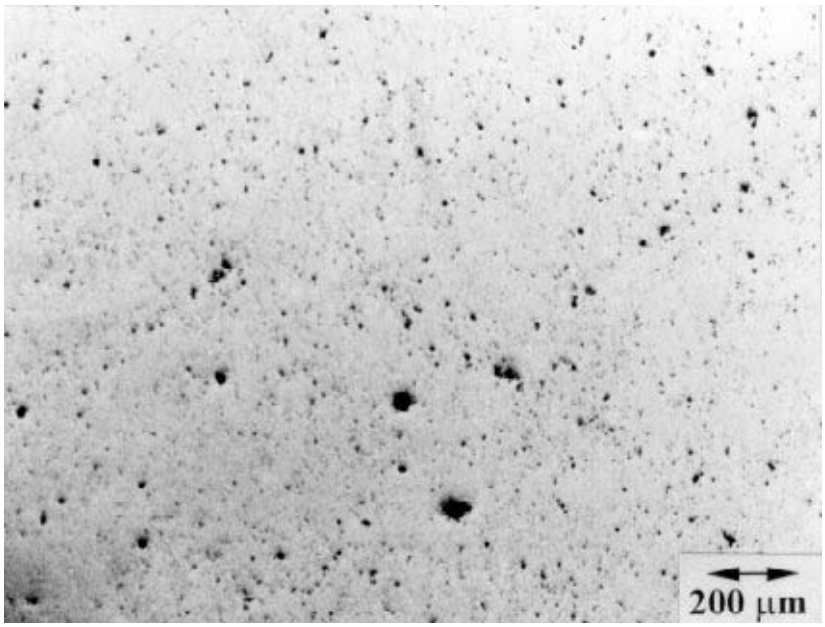

Fig.6: The uniform pore distribution in this hot-pressed amorphous Z40A sample is due to the removal of agglomerates larger than ~10μm. The indication is that hot-pressing finer amorphous powders (particles smaller than 1 μm) may eliminate all the porosity.

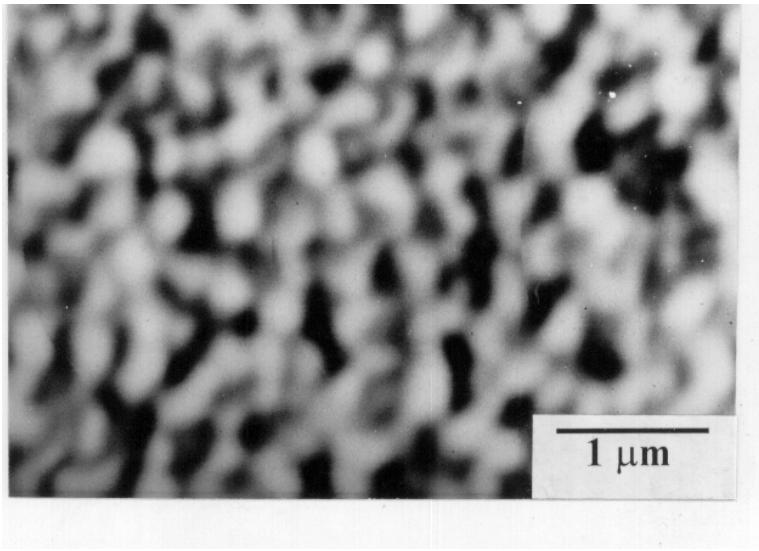

Fig.7: Controlled heat treatment of hot-pressed amorphous pellet can lead to a wide range of desirable microstructures. Scanning electron micrograph of sub-micrometer grains of m-ZrO_2 (bright phase) and α-Al_2O_3 produced by heating a dense amorphous pellet of Z40A to 1673 K for 1 hour.

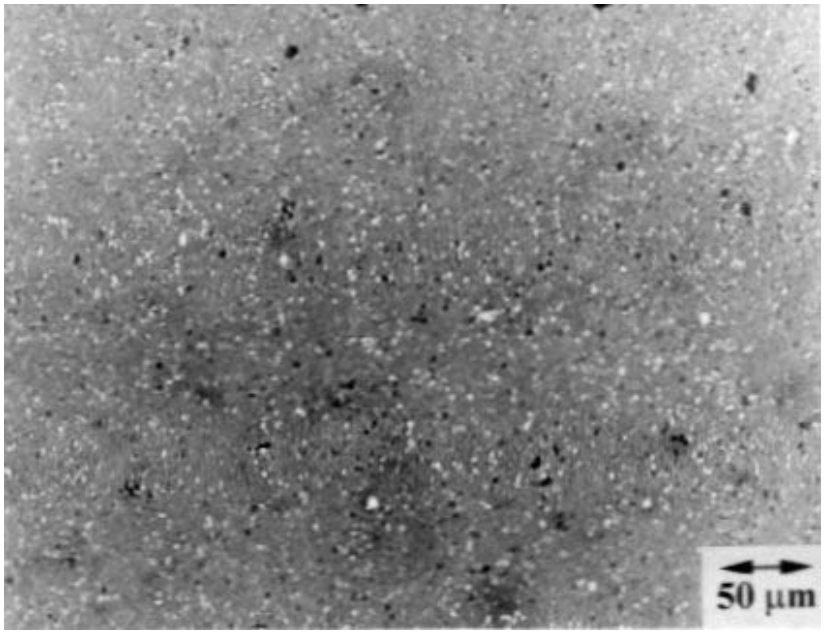

Fig.8: Optical micrograph of hot-pressed composite of amorphous ZrO_2-80 mol% Al_2O_3 reinforced with SiC particles (bright phase). This composite with only 1% porosity was produced at 923 K under 750 MPa pressure in air. Pores are randomly distributed whereas they surround the SiC in conventional processing[28,30].